The Response of Ocean Surface Layer to Rainfall

Jie Jiang

Rain falling on the ocean surface can form buoyant surface ‘lenses’ of fresh water, called ‘fresh lenses’. That will impose influences on the air-sea surface flux which can further affect global water cycle by the changes in SSS (Sea Surface Salinity), and on the modeling of upper ocean dynamics in rain-dominated regimes where salinity plays a significant role in determination of ocean vertical structures. Besides, due to the different measurement methods and depths between satellites and in situ drifters, such layer of fresh water can cause discrepancies among different observations, which will bring the issues of calibration and validation of satellite measurements of SSS. To address these problems, a more complete and profound understanding for the evolution of fresh lenses and their impacts on the vertical salinity structures is necessary. This article will first introduce the observational evidence of SSS decrease under rain events, work done by Boutin et al. (2014); later, a study on the evolution process of fresh lenses under varying conditions and fresh bias from satellite measurements by using Generalized Ocean Turbulence Model (GOTM) conducted by Drushka et al. (2015) is presented.

1. Observational Evidence of SSS Decrease under Rainfall

There are two satellite salinity missions that observe salinity from space: the soil Moisture and Ocean Salinity (SMOS) and the Aquarius missions. Since the L-band radiometry board on the satellites is only able to penetrate the first few centimeters of ocean while the in situ drifters Argo measurements taken at about 5 meters below surface, different SSS shall be expected and especially in rainy regions like Intertropical Convergence Zone (ITCZ), Southern Pacific Convergence Zone (SPCZ) and Indo-Pacific warm pool. Figure 1 gives the comparison between S_{1cm} measured by SMOS and S_{bulk} from Argo, with the information of rain rate (RR) at the same time period. It is clear the large differences from two observations likely to occur at areas where rainfall is common. More detailed analysis of how the SSS discrepancies are associated with RR is given as following.

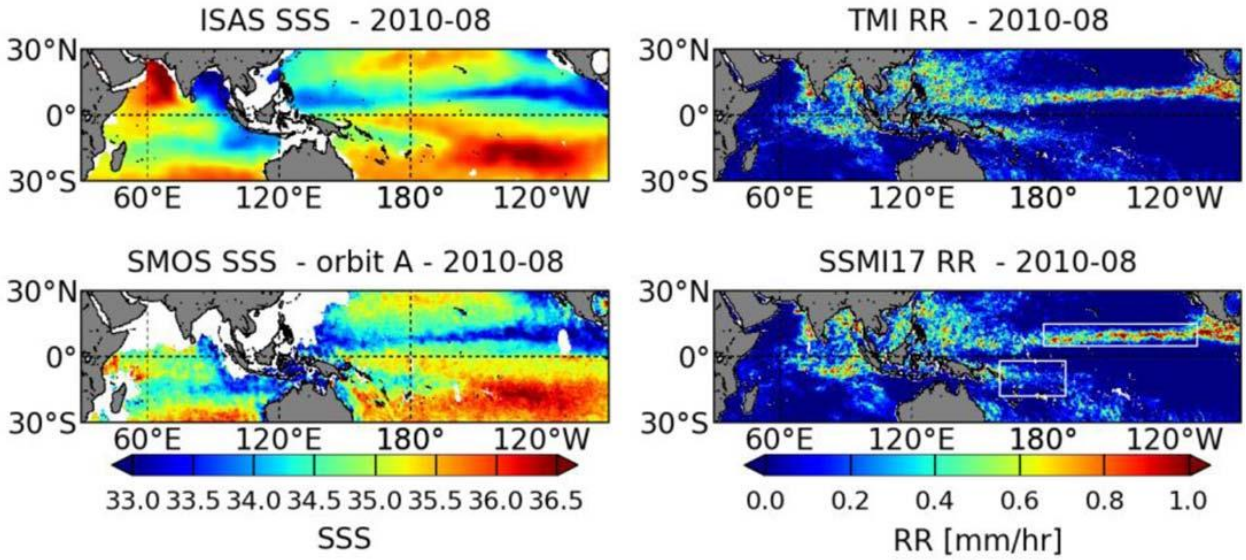

Figure 1 (left) SSS maps in August 2010 derived from (top) Argo measurements using the ISAS version of D7CA2S0 optimal interpolation at 5m depth (Gaillard, 2012); (bottom) SMOS measurements during ascending orbits (6 AM) (LOCEAN CEC CATDS 2013 product); (right) Rain rates derived from (top) monthly TMI measurements; (bottom) monthly SSMI F16 measurements with superimposed white boxes that indicate the regions in which we study SMOS-ARGO SSS differences.

1.1 Two Methods of Computing SSS Decrease

Since S_{1cm} detects the instant surface response to rainfall and S_{bulk} that measured at 5 meters down to the surface can be viewed as the salinity of mixed layer, thus the differences of salinity between the few centimeters depth and meters depth can serve as the SSS decreases. However, Argo S_{bulk} is also subject to rain events. Boutin et al. (2013) show the S_{bulk} taken under rainy conditions can be much fresher than the one measured later in non-rainy days, therefore, the S_{bulk} close to the time of rainfall is not a reasonable reference as bulk salinity. In order to avoid S_{bulk} influenced by fresh lenses, those measurements within -1h and +2h from rain events identified by TRMM3B42 are excluded. Nevertheless, the spatial and temporal coverage of Argo is much sparse than SMOS, thus a perfect match-up rarely exists and a compromise is made by assuming a time interval of ± 5 days and space interval of ± 50km in which the Argo S_{bulk} and SMOS S_{1cm} are comparable. Similarly, the RR of rain event captured by SSM/I satellite closest in time to the S_{1cm} measurement, within the interval of either -60min and +30min or -30min and +15min, is chosen.

The other method of assessing the SSS decreases is by comparing the spatial variability of SMOS S_{1cm}. In a measurement close to the time when rain events with RR larger than 5mm/h are detected, not only S_{1cm} within the range of 100km is documented, but SSS outside the rain cell within 150km from local S_{1cm} is averaged and viewed as equivalent to the surface salinity before perturbation by rain. Therefore, the differences between S_{1cm} taken at the rainy and neighboring non-rainy area can indicate the rainfall effects. This method has circumvent the temporal inconsistence existing in the first method discussed above but has the risk of underestimating the decrease in the cases that strong winds are present and thus significant horizontal advection may dilute the ocean surface within the rain-free region, or the fresh lenses resulted from rainfall may be mixed with salted water. Therefore, it would be better to discard the rain events in which strong winds are observed within the SMOS passes, especially around the lateral boundaries of rainy areas.

1.2 The Relationship between SSS Decreases and RR

The relationship between SSS decrease and RR in ITCZ at year of 2010 and 2012, deduced by SMOS S_{1cm} - Argo S_{bulk}, is shown in Figure 2. Generally, the SSS decrease is inverse proportional to RR, with slope of about -0.2 $\mathrm{pss}\,(\mathrm{mm}\cdot\mathrm{h}^{-1})^{-1}$. Because the SSM/I measurements were closer in time with SMOS ones, the

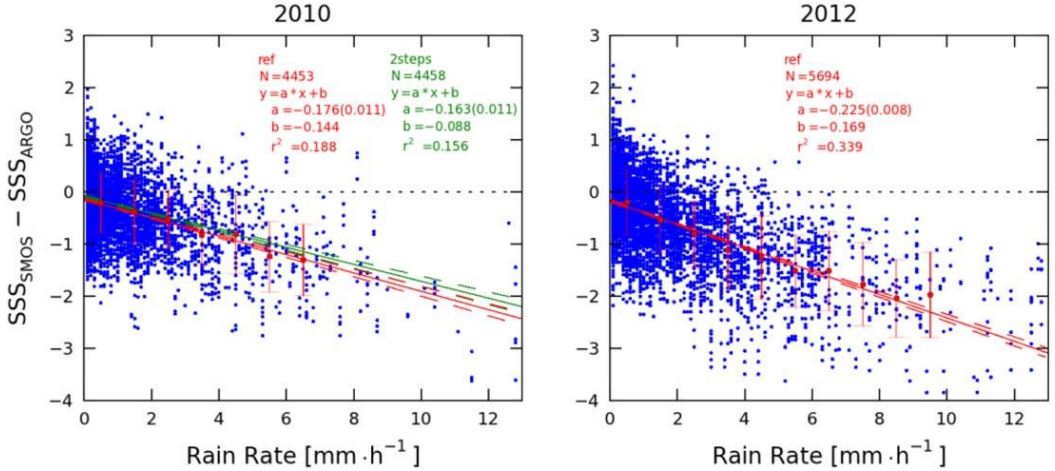

Figure 2 SMOS minus ARGO S versus SSM/I rain rate collocated within (230 min;115 min) in ITCZ region. (left) July–September 2010; (right) July–September 2012. The blue points correspond to individual SMOS SSS retrieved with the default algorithm. The red dots and bars indicate the mean plus and minus 1 standard deviation of SSS_{SMOS}-SSS_{Argo} within 1 mm/h RR classes provided classes contain more than 30 SMOS SSS. The corresponding fit (plain line) and its 95% confidence interval (dashed line) is plotted in red. On figure left, we have also superimposed the fit and 95% confidence interval obtained from SMOS SSS retrieved with the two step algorithm (green).

response of surface salinity captured by satellite to rainfall will be more immediate and direct. Hence the correlation between them and magnitude of the slope in 2012 is slightly greater than the ones of 2010. It should be noted that the differences between the satellite measurements and in situ observations will not only be contributed by the sea surface salinity itself, but also can be influenced by other factors such as atmospheric effects (which has been proved to be small but not discussed here), vertical stratification and surface roughness. In order to distinguish the consequences from various sources, two retrieval algorithms for retaining S_{1cm}, namely the operational retrieval algorithm (reference algorithm) and the two step retrieval algorithm, have been adopted at 2010. The latter one has estimated SSS with better quality, by correction of the differences between ECMWF wind speed and SSM/I radiometric wind speed without too much noise, which is associated with the surface roughness. In other words, the two step retrieval algorithm could refrain the measurement of SSS from influence of the surface roughness induced by rainfall. However, the results out of these two algorithms don't present significant differences (Figure 2, left), which indicates that the rain-roughness effect is likely to occur but is a second order effect (less than 8% of the total rain effect) with respect to the SSS decreases.

The spatial variability of S_{1cm} observed to the rain cells is very well correlated with rain rates, provided that the temporal lag between the SMOS SSS and satellite RR is short. In a particular case, in the northern subtropical Atlantic region on 26 August 2012, Boutin et al. (2014) argued that the effect of rain on SMOS SSS is -0.18(± 0.019) $\mathrm{pss}\,(\mathrm{mm}\cdot\mathrm{h}^{-1})^{-1}$, which is very close to the outcome from the comparison between SMOS S_{1cm} and Argo S_{bulk}.

To test the validity of this relationship, a removal of rain effects ($\approxeq -0.2\,\mathrm{pss}\,(\mathrm{mm}\cdot\mathrm{h}^{-1})^{-1}$) is applied to the monthly maps of SMOS SSS, which can be mathematically expressed as $S_{1cm}' = \overline{S_{1cm}} + 0.2\cdot\overline{RR}$ where $\overline{RR}$ represents the monthly mean of interpolated rain rates. This correction should suppress the rain-induced variability. Nevertheless, it has been shown that the correction accounts 40% at most for the $\overline{S_{1cm}} - \overline{S_{bulk}}$ and it only slightly reduces the variability of SSS. Other factors may explain the differences including the spatial interpolation of measurements which smoothes the spatial gradients, relaxation to SSS climatology in the mapping algorithm which could overestimates SSS in rainy region etc.

Boutin et al. (2014) argue that based on the coarse data resolution and insufficient matchups between observations of rain events and SSS measurements, a reliable conclusion can't be made. Indeed, although their results have verified the existence of the fresh bias of satellites compared to in situ observations of sea surface salinity, and provided some useful insights of the possible relationship between the SSS decrease and RR, there are several indispensable flaws in the data analysis. The fundamental disadvantage of this study, as the authors have said, is lack of simultaneous comparisons between SMOS S_{1cm} and Argo S_{bulk}, SSS and RR, which is owing to the sparse sampling. Besides, in addition to the instant rain rates, the accumulation effects of fresh water from rainfall should be considered as well, which is prevented by the low time resolution of data in this case. Finally, a more comprehensive study on the factors committing to the response of ocean surface to rain may take the surface wind stress and background ocean stratification into account.

2. The Evolution of Fresh Lenses Simulated by GOTM

The layer of fresh water produced by rainfall will change SSS and thus increase the vertical salinity gradients, making the surface layer more stable, suppressing the transfer of momentum and heat. But this structure will eventually be interrupted by horizontal advection, vertical mixing and convectively driven overturning during nighttime cooling. Both SSS and the depth of mixed layer will change during the evolution process. However, due to the infrequence and transience of rainfall, it is difficult to observe and record those parameters featured during the lifetime of rain-induced fresh lenses. Therefore, employing a proper ocean model to study the continuous development seems to be a good choice. In this section a brief description of GOTM is given first, followed by the verification of model performance, then a discussion about the evolution of fresh lenses under varying conditions through sensitivity experiments is presented,

and the last section will compare the model results of yearlong GOTM simulation with annular averaged observation data.

2.1 Model Description

GOTM is a one-dimensional water column model that computes solutions for the vertical transport equations of heat, salt and momentum. For the future purposes of model performance verification, of reproduction, and of consistence between different variables, it is reasonable to settle the external forcing and initial conditions as similar to the observational data. But once the model is proved to be valid and efficient, then sensitivity experiments can be carried out by setting idealized values, which will be discussed later. In terms of external forcing, rain rate, RR; zonal and meridional wind speeds, U_Z and U_M; solar radiation, I_S; air temperature, T_A; relative humidity, RH; barometric pressure, P_A; and cloud fraction, C, are required. Satellite and reanalysis data products are used for yearlong GOTM simulations. Rain rate estimates come from NOAA Climate Prediction Center morphing method (CMORPH) product, and other meteorological forcing (U_Z, U_M, T_A, RH and C) are obtained from ERA-Interim global atmospheric reanalysis product by the European Centre for Medium-range Weather Forecasting (ECMWF). Absorption of solar radiation is calculated by the model itself according to the latitude, time of the day and the cloud fraction. As for the initial conditions, consisted of the vertical profiles of ocean temperature T and salinity S, are obtained from a gridded Argo climatology. The shallowest depth of Argo measurements is 5 meters, so T and S between 0 and 5m are set to Argo 5m values, implying a well-mixed bulk ocean surface layer. Vertical velocity profiles of zero are used.

2.2 Model Validation

Two observation events of rainfall featured by high temporal resolution and high vertical resolution separately are used to verify the validity of GOTM. The meteorological parameters either serve as external forcing or initial conditions are equal to the observations during the rain. The first observation is conducted by SSP, a towed and surface-following platform equipped with four conductivity-temperature-depth sensors (CTDs) to sample T and S at the depth of 0.11, 0.26, 1.0 and 2 meters, which collects data under a moving frame of reference. Owing to the insignificant spatial variability of rainfall, one can assume that the spots within the rain field are subject to the similar evolution process, and the measured spatial variability is equivalent to that would be measured at fixed point. Therefore, the time series of T and S presented in Figure 3b is used here, where the time from the start of the rain is computed as the distance from the maximum rain rate divided by the speed over ground of the ship. Figure 3a depicts the wind speed and RR as a function of time, and a maxima of rainfall occurs at around 13:10 local time followed by a rapid drop of salinity near surface (salinity at 0.11m and 0.26m) then it gradually recovers. Though the salinity at deeper ocean rarely change over this period it ultimately decreases slightly due to vertical mixing. Figure 3c shows the model salinity at the same depth levels as the four SSP sensors. GOTM reproduces the salinity response well, including predicting the magnitude of the anomaly at each depth and the erosion of the salinity gradients at the end of the rainstorm. The time it takes for the fresh anomaly to

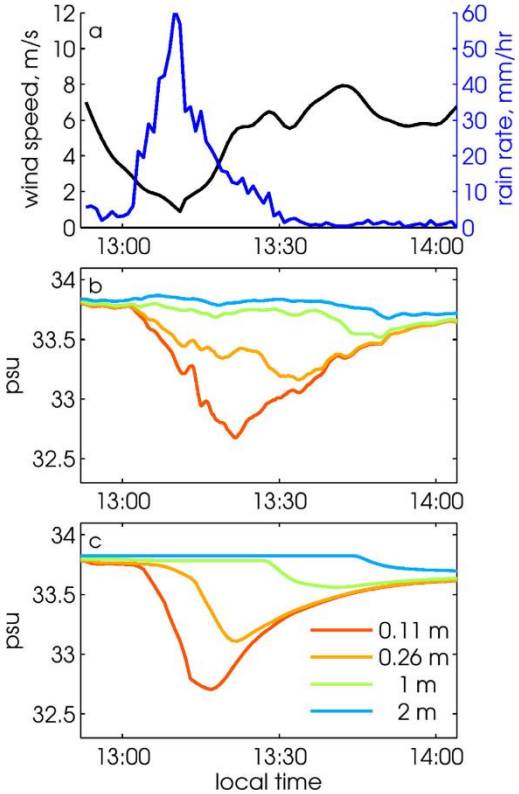

Figure 3 Observed and modeled rain event from the central Pacific Ocean. (a) Ship-based measurements of wind speed and rain rate made in 2011. (b) Salinity at four depths measured by the SSP. (c) GOTM simulation of salinity at the same four depths.

propagate downward, which is seen as the lag between the peak salinity anomaly at each depth is also reproduced fairly well, though it appears earlier in the model. The high-frequency signal in observation is likely to be a result of existing variability in small-scale ocean structure or spatial/temporal variability in the rain field.

The other field observation is carried out by the Air-Sea Interaction Profiler (ASIP), which gives high-resolution vertical profiles of T, S and TKE dissipation ϵ, from below the base of the mixed layer to the sea surface. Figure 4 presents the observations of surface wind, RR, vertical salinity and dissipation rate as well as the model outcomes. The rain has formed a freshwater layer of nearly 2m deep when rainfall deceases. A sharp decline in dissipation rate below the base of the fresh lenses appears once the layer forms, elucidating the resulting stratification effect from the strengthening magnitude of vertical salinity gradient on the suppression of turbulence. The model has given a correct estimate of the depth and the lifetime of fresh water, successfully predicted the sudden change of dissipation rate though kind of greater at the last time of observation period.

Besides the capacity of reproduction under certain settings, it's also important to test the stability of the model given that different conditions. It has been proved that the model is not sensitive to the choice of time step, domain depth or vertical grid spacing within a reasonable range of values. Although lateral advection should be non-negligible in real ocean, the one-dimensional model has demonstrated its reliability in understanding the dynamics of freshwater lenses in the cases of large scale and weak horizontal currents.

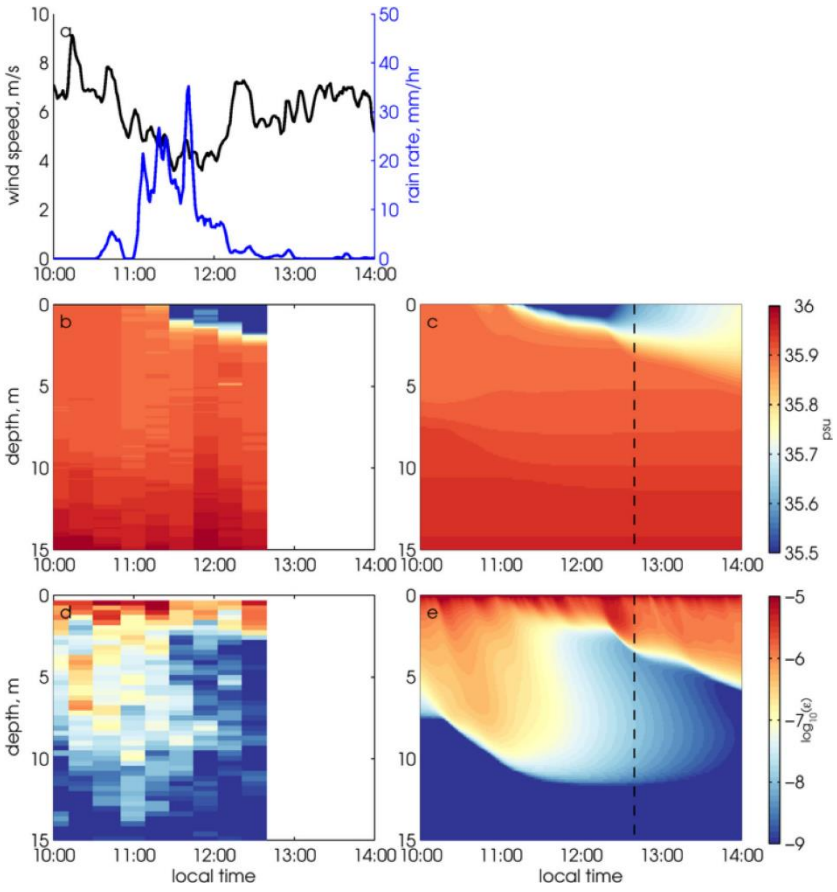

Figure 4 Rain event observed in the North Atlantic Ocean in 2011. (a) Ship-based measurements of wind speed and rain rate. (b) Salinity profiles measured by ASIP at the rate of one profile every 18 min. (c) Salinity profiles from GOTM simulations. (d) Dissipation rate profiles (log scale) measured by ASIP. (e) Dissipation rate profiles from GOTM simulation.

2.3 Factors Contributing to the Evolution of Fresh Lenses

Similar to what Boutin et al. (2014) have done before, Drushka et al. (2015) intend to find out the qualitative relationship between SSS decrease and contributing factors first by analyzing observational dataset. By doing so, a crude guess of their relationship can be established which will provide the basis for determination of uncertainties by delivering ideal sensitivity experiments. Drushka et al. (2015) compute the salinity differences at depths of 0.86m and 2.1m, at which are the shallowest levels the CTDs aboard a mooring in the Atlantic Ocean detect. The maximum rain rate R_{max} and the maximum absolute difference ΔS_{max} are picked out to represent the intensity of a rainfall and a metric for the strength of the vertical salinity gradient formed by that rain event. There are total 134 events taken into account, by excluding those with large

horizontal advection which are not entitled to be studied with one-dimensional model, and those with too small ΔS_{max} that exceed the limit precision of detection. Figure 5 shows the distribution of these events in U- ΔS_{max} space, where the color denotes the rain rate. Although points are scattered, the inverse relationship between ΔS_{max} and wind speeds as well as the positive correlation between ΔS_{max} and R_{max} can be clearly seen.

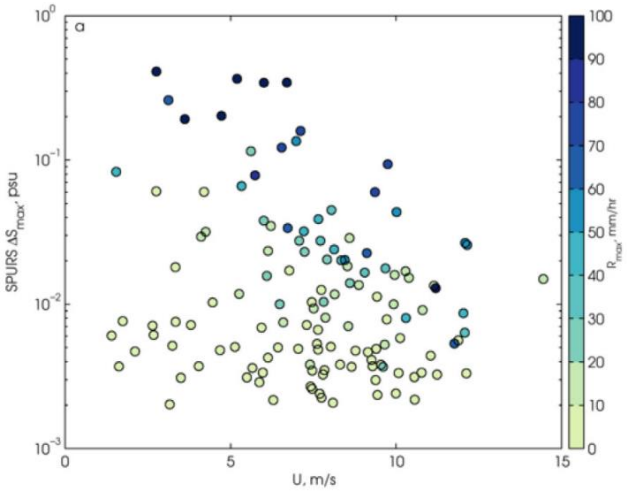

Figure 5 (a) ΔS_{max} between 0.86 and 2.1 m as a function of wind speed for events observed at the SPURS mooring in the subtropical North Atlantic Ocean.

Once the validity of GOTM on prediction of the development of rain-induced freshwater layer has been proven, the model can be used to explore and verify how rain intensity, wind forcing, and background ocean conditions affect the formation and evolution of fresh lenses. Contrary to working on limited observational rainy cases with imperfect even incorrect matchups of information, huge complexity in background conditions and limitation of examining impacts from factors like the temporal distribution of rainfall and accumulation effects of rain, model simulations can provide much more possibilities to facilitate the study. One can adjust external forcing flexibly to meet the requirements for certain purpose. The numerical experiments are initiated with ocean conditions from the SSP deployment (see Figure 3), and are forced with constant wind ranging from 1m/s to 10m/s (zonal and meridional components are set to the same value), a Gaussian pulse of rain having a prescribed R_{max} lasting for one hour (defined using the full width of the Gaussian at on tenth of the peak) with maxima at 0900 local time. Other meteorological parameters T_A, RH, and P_A are held fixed using the average value from the SSP observation and C is set to 100% over the entire simulation period. Such setting can assure the ocean response is directly due to rainfall. Initial T and S profiles came from the gridded Argo dataset at the location the SSP measurements are made, and are shifted to match surface T and S observed with the SSP. In order to distinguish the diurnal effects from rainfall effects, a control model run without rain at each wind speed is carried out.

Here, several parameters are derived to characterize the ocean response and to simplify intercomparison of model runs. The thickness of the lenses, D_L, is defined as the depth at which salinity anomaly relative to no-rain control run is 10% of maximum anomaly. The lifetime of the lens, T_L, is the time over which D_L is nonzero. Finally, in order to relate the model findings to satellite-Argo salinity comparisons, the difference in S between 0.01(i.e., roughly the depth of L-band satellite measurements) and 5m (i.e., roughly the depth of the uppermost Argo measurements) is calculated at each time step, which is denoted as ΔS, the 5m salinity subtracted from 0.01m salinity. What we are most interested here is the maximum magnitude of the vertical gradient over the lifetime of lenses, ΔS_{max}, which is always positive.

The results from the sensitivity runs are summarized in Figure 6. Unsurprisingly, at a given wind speed the vertical gradient is nearly proportional to the maximum intensity of rainfall as heavier rain can cause much more significant dilution process across surface layer and leading to stronger vertical salinity contrast. When given at a certain rain rate, ΔS_{max}, T_L are inversely dependent on wind speed while D_L is positive related to U, since stronger winds can enhance vertical mixing, transfer fresh water from surface into deeper ocean thus the depth of fresh lenses will increase accordingly, but the vertical gradients will be reduced and the structure can't maintain long. The ocean vertical structure formed under strong winds are featured by small ΔS_{max}, large D_L, and T_L of a few hours at most. In contrast, rainfall during weak winds produce a fresh lens with a large ΔS_{max}, small D_L, and T_L on order of 10h. Based on the results showed in Figure 6, a linear proportional relationship between ΔS_{max} and R_{max} can be expected and after performing

a least squares linear regression of ΔS_{max} with respect to R_{max} at each U, it emerges that the slope of each line is inversely proportional to U. Therefore, ΔS_{max} can be expressed as a function of R_{max} and U as following:

$$\Delta S_{max} = A R_{max} U^{-b}$$

where the constants A and b differ at different regions and will be determined from fitting procedures. Using all GOTM runs, with the background ocean and atmospheric conditions from the central Pacific ocean, these coefficients are found to be $A = 0.11 \pm 0.03\,\mathrm{psu}\,(\mathrm{mm \cdot h^{-1}})^{-1}$ and $b = 1.1 \pm 0.03$. One of the greatest improvements of the theory of Drushka el al. (2015) compared to that of Boutin et al. (2014) is the former have taken the wind speed into consideration. Although the equation for ΔS_{max} presented above is stemmed from sensitivity experiments of model simulations, it is more reasonable to address the coefficients with observational dataset.

Figure 6c shows the influences of winds and rain rates on the maximum depth of fresh lenses during their lifetime. Fresh lenses deepen along with the increase of wind speeds, but slopes are dependent on the rain intensity. When rain rate is 50mm/h, every time the winds strengthened by 2m/s it will make the fresh water penetrate 1.25m deeper into the interior ocean, while the rain rate reduces to 2mm/h the winds can't impose such significant influences to the fresh lenses as before and the depth of fresh water seems to have a upper limit. This phenomenon may be explained by the volume of fresh water brought by rainfall, since deep water column is impossible to form if there isn't sufficient water available no matter how strong the winds can be. In terms of how long the layer of fresh water can persist, vertical mixing caused by surface winds

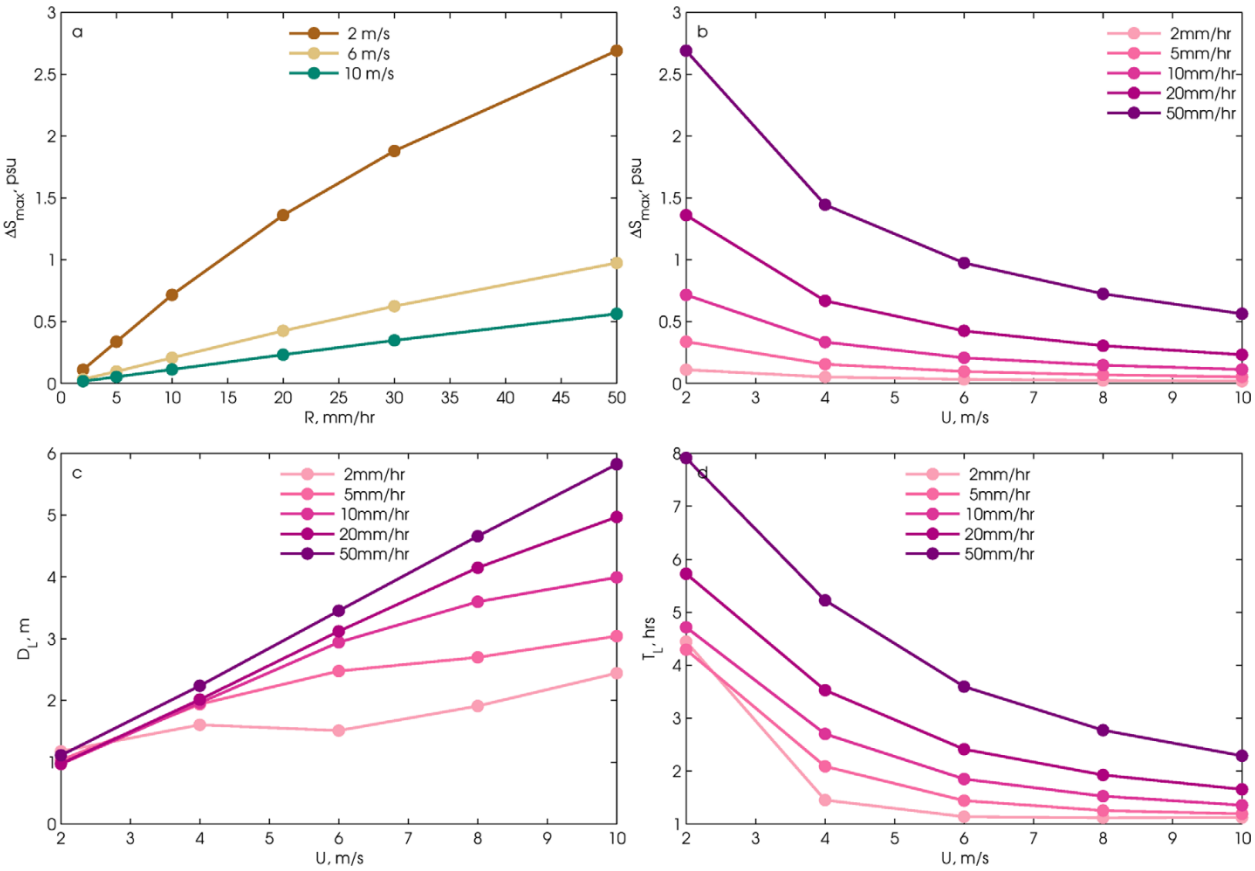

Figure 6 Results from the GOTM experiments using idealized environmental forcing functions in which the peak rain rate and the wind speed were varied. (a) Peak magnitude of ΔS, ΔS_{max}, as a function of rain rate, for three different wind speeds; (b) ΔS_{max} as a function of wind speed, for different rain rates; (c) maximum thickness of the fresh lens, D_L, as a function of wind speed at different rain rates; and (d) lifetime of the fresh lens, T_L, as a function of wind speed at different rain rates.

will shorten its lifetime. For example, when $R_{max} = 50\,\text{mm/h}$, $T_L = 8\,\text{h}$ for $U = 2\,\text{m/s}$. In contrast, $T_L = 2.5\,\text{h}$ for $U = 10\,\text{m/s}$. At constant U, smaller values for R_{max} result in smaller T_L, as the lens disperse more quickly when less freshwater is deposited.

So far, we have used the maximum rain rate as the instrument to describe a rain event, but it is possible that total rainfall accumulation, as opposed to R_{max} that drives the salinity response. Therefore, a series of control experiments having the same amount of rainfall (0.01m) but different duration time (ranging from 30min to 6h) thus different maximum rain rate is performed to test the sole role of freshwater amount on the evolution of ocean surface layer. Figure 7 shows that although same amount of water is deposited in all experiments, ΔS_{max} varies much and is obvious related to the R_{max}. Interestingly, T_L is approximately the same for each event, and recall what we have discussed before that T_L is greater when the maximum rain rate is larger thus the total accumulation of rainfall is also larger when the duration of rainfall remains constant among all the experiments. It indicates that T_L, unlike ΔS_{max}, is dominated by the total volume of fresh water applied to the ocean rather than R_{max}. If the lifetime of fresh lenses is important (e.g., when considering the reduction of turbulence below the lens), more attention should be appointed to the accumulation effects of rain; if the vertical gradients of salinity is desired (e.g., the impacts on satellite-Argo salinity bias), then R_{max} is more salient metric than T_L.

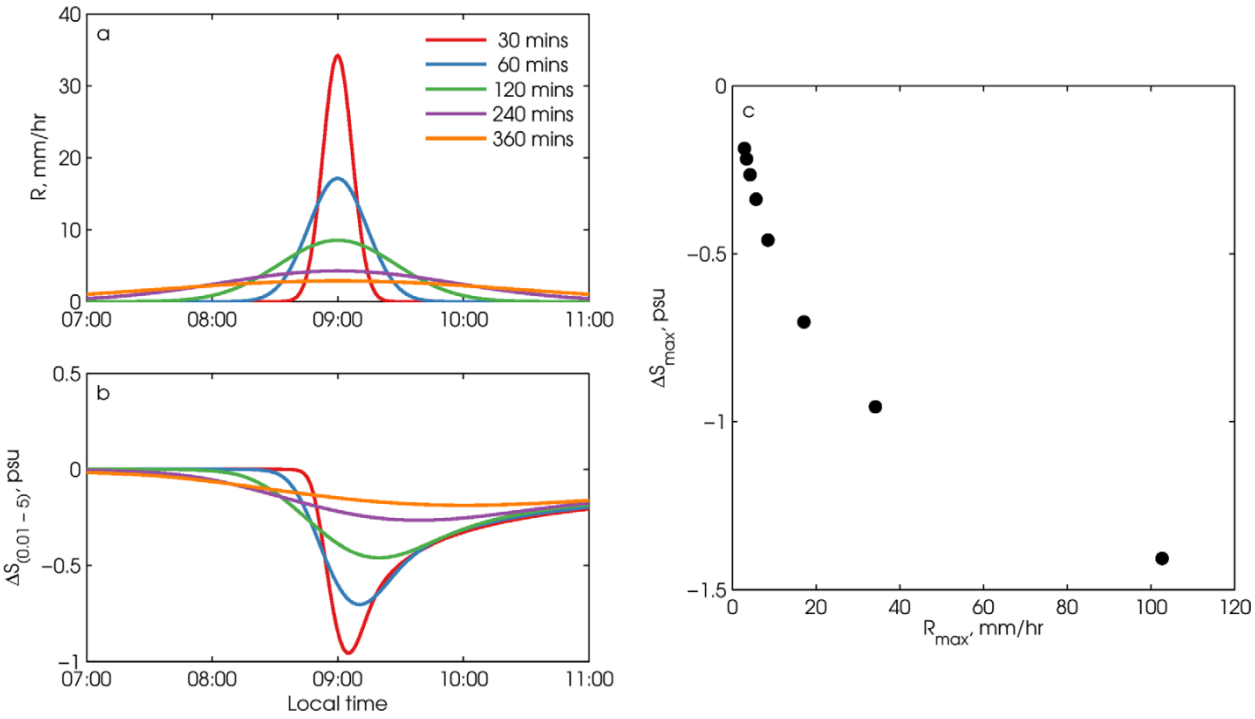

Figure 7 Results from GOTM experiments using idealized environmental forcing in which the same total rainfall accumulation of 0.01 m was applied, but the time over which it was applied varied in each case (indicated in the legend). (a) Rain rate as a function of time; (b) ΔS between 0.01 and 5 m as calculated from the GOTM simulations for the rain rate time series in Figure 6a; (c) ΔS_{max} plotted as a function of R max for all conditions.

Besides, we have assumed the temporal distribution of rainfall is Gaussian, and the effect of a non-Gaussian distribution is studied by running simulations where rain rate is a constant value for a finite length of time. Although the resulting rain lenses had a slightly different shape in comparison to the lenses formed using Gaussian rain pulses, ΔS_{max} has a similar relationship to U and R_{max} as it did for the hour-long Gaussian rain cases. This suggests that it is R_{max} rather than the duration of the rain event or temporal profile of R, that determines ΔS_{max}. It should be noted that here all the experiments are designed to take place at the midmorning when the ocean surface layer become stable after the absorption of solar radiation, but the

results may be different when the background stratifications change either due to the diurnal cycle or the influences of weather systems.

Additional sensitivity experiments are performed to explore how upper ocean temperature and salinity conditions affect ΔS_{max}. At a given temperature, the near surface anomaly resulting from rainfall is proportional to the initial surface salinity, which can be explained by the following equation:

$$\Delta S = \frac{m_{salt}}{m_{water}} - \frac{m_{salt}}{m_{water} + m_{rain}} = S \cdot \frac{m_{rain}/m_{water}}{1 + m_{rain}/m_{water}}$$

Where m_{salt}, m_{water}, m_{rain} is the mass of dissolved material, ocean water and rain respectively. Therefore, rain falling on saltier water will generate a stronger vertical salinity gradient than fresher water. At a fixed surface salinity, the impact of SST on ΔS_{max} is found to be small, with the magnitude of ΔS_{max} decreasing slightly with increasing temperature.

2.4 Implication of Rain-Formed Fresh Lenses for Satellite Validation

Previously, Boutin et al. (2014) compared satellite and Argo salinity measurements as a function of R to determine if rain-induced vertical stratification between the surface and a few meters causes a fresh bias between satellite-derived and Argo-derived salinities. Although the study is limited by the relatively sparse spatial and temporal overlap between Argo profiles and satellite overpasses, it suggests that there is fresh bias during rain events. However, Drucker and Rise (2014) also point out that the rain events may be too infrequent to cause a significant fresh bias in long-term average. To compensate for the limitation of previous studies, model simulations allow a more detailed analysis, from which the rain-induced fresh bias in long-term average satellite salinity can be estimated by the differences between the model salinity at 0.1m and 5m depth.

The yearlong simulation of one-dimensional GOTM is forced by the rain data from CMORPH and wind vectors, RH, T_A, P_A, and C from ERA-Interim data, over the region of 20° S-20° N with grid resolution of $0.25° \times 0.25°$ using a 5min time step from Jan.1 to Dec.31 2012, and in order to make up for the horizontal mixing a procedure of relaxing the vertical salinity profile to the climatologic conditions is conducted every week. Through sensitivity tests, it emerges that lack of horizontal advection can result in overestimates by 50%, on the contrary missing high-frequency winds and rainfall may lead to underestimates. Figure 8 depicts the comparisons among the model yearlong averaged outcome, 0.1m salinity of Aquarius subtracted of 5m salinity of Argo observation and 0.1 salinity of Aquarius subtracted of 1m salinity of HYCOM reanalysis data. All results have witnessed magnificent fresh bias at regions having heavy rainfall but weak winds like eastern Pacific, Atlantic ITCZ, SPCZ region and throughout the tropical Indian Ocean outside of the Bay of Bengal. However, there exits inconsistence as well. The western equatorial Pacific region shows a prevalent fresh bias in yearlong averaged patterns from both GOTM ΔS_{mod} and Aquarius-HYCOM ΔS_{hyc}, but a salty bias in Aquarius-Argo ΔS_{obs}. And both in the Indian Ocean and central Pacific Ocean south of 10°S where strong winds and low rain rate are dominant, there is a strong fresh bias in Aquarius compared to both Argo and HYCOM but ΔS_{mod} is near zero. It is not clear that if those differences are due to problems in the model or the relative paucity of observational data leading to undersampling of the surface freshening, or if they could result from interannual variations that are represented in the observations but not by the yearlong model run.

3. Summary

Two articles (Boutin et al., 2014; Drushka et al., 2015) discussed here present an explicit course starting from a crude conclusion by dealing with observational dataset to a more complete and reliable theory using valid numerical model. Observations and simulations compensate and implement for each other, as less unconstraint and flexible model simulations can make up for the limitation of observations due to relatively

sparse data sampling while realistic observations can initiate, force and verify the simulations. Such cooperation can greatly develop the understanding towards an unsolved natural phenomenon.

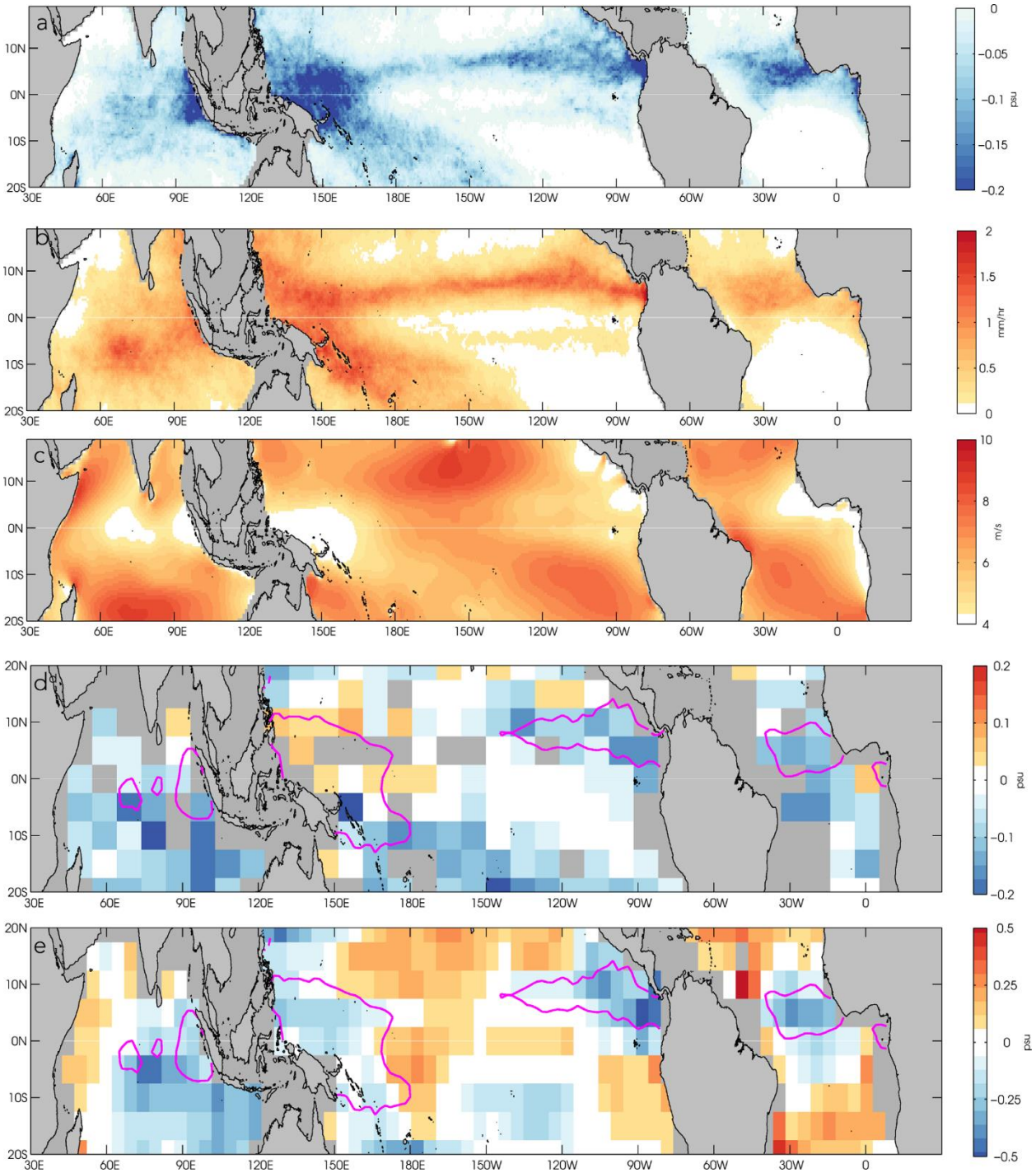

Figure 8 $\overline{\Delta S_{mod}}$, the annual average of DS between 0.01 and 5 m, calculated from GOTM experiments run at each grid point for a 0.58 3 0.58 grid. (b) Mean rain rate, based on CMORPH precipitation estimates from 2012 on the same grid as Figure 7a. (c) Mean wind speed, based on ERA-Interim winds from 2012. (d) $\overline{\Delta S_{obs}}$, the average difference between salinity from Aquarius and from Argo at 5 m (negative indicates that Aquarius measures a fresher value). Individual Aquarius-Argo pairs were averaged to a 108 longitude 3 58 latitude grid. (e) $\overline{\Delta S_{hyc}}$, the average difference between Aquarius and HYCOM salinity at 1 m depth. The pink line in Figures 7d and 7e is the 0.08 psu contour of $\overline{\Delta S_{mod}}$ from Figure 7a.

To address how the ocean surface salinity change after rainfall, Boutin et al. (2014) propose two methods to quantify the salinity decrease. One is calculating the spatial variability of SMOS S_{1cm} measured at few centimeters depth, assuming the neighboring sea surface salinity outside the rain cell as the reference value, which is used to compare with the one under the mercy of rain. The other takes the differences between the sea surface salinity and the bulk salinity of mixed layer by matching SMOS overpasses to in situ observations Argo S_{bulk} that measure the salinity at 5m depth. Besides the salinity decrease, rain rates from observations of SSM/I are documented as well and are be associated to the salinity decrease. The results from both approaches indicate the rain-induced salinity decrease is larger when rainfall is stronger, which approximately presents a linear relationship with coefficient of -0.2 $\mathrm{psu}(\mathrm{mm}\cdot\mathrm{h}^{-1})^{-1}$. However, when eliminate the effects of rain-induced salinity differences from the monthly averaged total differences between SMOS and Argo, there still remains 60% discrepancies can't be explained. Although this study is seriously limited by the paucity of data which leads to poor spatial/temporal resolution, incorrect matchups and interpolation errors, it still provides some illuminating insights about the possible relationship between salinity changes and rain rates, as well as the satellite bias in terms of ocean salinity.

Based on the work of Boutin et al. (2014), Drushka et al. (2015) has taken a further step by employing the one-dimensional Generalized Ocean Turbulence Model (GOTM). The model is initiated and forced by in situ observation or reanalysis data. Before getting down to model simulations, they have analyzed the observation data from SPURS mooring in the subtropical North Atlantic Ocean, and unlike Boutin et al. (2014) who only categorize wind speeds into three rough classes, Drushka et al. (2015) have taken winds into more detailed consideration. They found that the salinity differences are not only related to the rain rates but will become smaller when the winds speed up at a given rain rate. After the verification of model performance, they have conducted a series of sensitivity experiments to study the ocean response to rainfall when horizontal advection can be neglected. Three parameters are invented to quantitively describe fresh lenses, namely the maximum vertical salinity difference ΔS_{max}, the depth of fresh lens D_L, and its lifetime T_L. The results suggest that ΔS_{max} is linear proportional to R_{max} with the slope of $0.11 \pm 0.03\,\mathrm{psu}(\mathrm{mm}\cdot\mathrm{h}^{-1})^{-1}$ in central Pacific Ocean but is inverse proportional to wind speeds U. D_L is found to have similar relationship with R_{max} and U. As for the duration of fresh lenses, it emerges that instead of the maximum rain rate it is the accumulation effects or the total amount of freshwater volume that matters. Although a Gaussian distribution is adopted first, it has been verified that the temporal distribution has little impacts. By deploying numerical simulations, factors including rain rates, wind speeds, accumulation effects of rainfall and temporal distribution have been examined, but all the experiments are built under stable stratification and the conclusion could be more precise if various background vertical ocean structures are considered such as unstable structures which are likely to occur during night and early morning. Finally, Drushka et al. (2015) use model salinity differences between 0.1m and 5m to reproduce the differences between satellite Aquarius and Argo measurements. It has successfully estimated the fresh bias in regions of frequent rainfall but low-speed winds like ITCZ, SPCZ and tropical Indian Ocean but there still exits inconsistence and causes responsible for that are not clear for now.

References

Boutin, J., Martin, N., Reverdin, G., Morisset, S., Yin, X., Centurioni, L., and Reul, N. (2014), Sea surface salinity under rain cells: SMOS satellite and in situ drifters observations, *J. Geophys. Res. Oceans*, 119, 5533– 5545, doi:10.1002/2014JC010070.

Drushka, K., Asher, W. E., Ward, B., and Walesby, K. (2016), Understanding the formation and evolution of rain-formed fresh lenses at the ocean surface, *J. Geophys. Res. Oceans*, 121, 2673– 2689, doi:10.1002/2015JC011527.